RSC Advances

PAPER

Cite this: *RSC Adv.*, 2019, **9**, 10135

An antibacterial and biocompatible piperazine polymer

Maolan Zhang, †[a] Guoming Zeng,†[a] Xiaoling Liao[a] and Yuanliang Wang*[b]

Bacterial repellence by biomedical materials is a desirable property that can potentially improve the healing process. In this study, we described a simple and green method to prepare a novel piperazine polymer (PE), which was based on the raw materials piperazine (PA) and ethylenediaminetetraacetic dianhydride (EDTAD). The structure and thermal stability of the obtained material were characterized using Fourier transform infrared spectrometry (FTIR), nuclear magnetic resonance spectroscopy (NMR), elementary analysis, differential scanning calorimetry (DSC) and thermogravimetric analysis (TGA). To evaluate the antibacterial properties of PE, a strain of Gram-negative *Escherichia coli* (*E. coli*) bacteria and a strain of Gram-positive *Staphylococcus aureus* (*S. aureus*) bacteria were used. The results indicated that PE exhibited good antibacterial activity against both strains of bacteria in a short time frame. The initial cytotoxicity test of the obtained material was based on the changes in the morphology and proliferation of osteoblasts, and the results demonstrated that the cytotoxicity of PE was concentration-dependent. Combining the experimental results of these two parts, it was shown that bacteria could be inhibited by a certain concentration of PE, while its toxicity toward osteoblasts was very low. In summary, these results revealed the potential usefulness of PE in biomedical applications.

Received 22nd March 2019
Accepted 25th March 2019

DOI: 10.1039/c9ra02219h

rsc.li/rsc-advances

1. Introduction

Bacterial contamination is a highly vexing problem that has attracted serious concerns globally.[1–3] Microorganisms can colonize on a wide variety of surfaces, including wound dressings, food packages or medical devices, and this colonization may lead to the formation of a biofilm. A so-called biofilm results from the accumulation of organic molecules, metabolites and microorganisms, providing an ideal shelter for the bacteria inside. Therefore, these bacteria could become resistant to the host immune system, as well as to antibiotic treatment.[4–6] Since the biofilms are so difficult to remove, the only effective way to deal with a biofilm-induced infection is to completely replace it with a new one. However, this is extremely inconvenient and costly. Therefore, it is highly desirable to find methods to resist bacterial adhesion or even kill the bacteria. This strategy focuses on preventing the biofilm formation at the initial stage. In the published literature, there are two primarily strategies. One strategy is to design an antibacterial surface,[7–10] and the other is to use antimicrobial agents.[11–14]

Various surface modifications have been developed to improve their antibacterial properties, such as functionalization with bacteriostatic groups or bactericidal agents.[15] The more commonly used antimicrobial materials in this field include the following categories: quaternary ammonium salts, phosphonium salts, metal ions, or even antibacterials such as ciprofloxacin, *et al.*[16–19] However, most of these antibacterial materials have some problems, such as high costs, complicated production processes, low durability, residual toxicity or a rapid increase in bacterial resistance that render them ineffective within a few years.[20,21] Compared with these traditional small molecule antibiotics, antibacterial polymers have unique advantages. There are two antibacterial polymers that are worth mentioning. One of which are natural occurring antimicrobial peptides (AMPs), which are well known for much lower levels of bacterial resistance. However, these are costly, undergo proteolytic degradation and are synthetically challenging.[22–25] The other is chitosan (CTS). As one of the most important and abundant natural polysaccharides, CTS demonstrates excellent performance, is biocompatible and nontoxic, and exhibits antimicrobial activity.[26,27] However, CTS is limited by its poor solubility.[28] Therefore, it is necessary to develop various facile methods to produce novel polymers with simple syntheses, good antimicrobial activity, solubility and biocompatibility.

Due to its unique physicochemical characteristics and biological activities, PA and its derivatives have been widely investigated for applications in chemical industry, especially in the field of medicine. PA and its derivatives have been used to synthesize antibacterials (such as ciprofloxacin), antibiotics,

[a]*Chongqing University of Science and Technology, Chongqing 401331, China. E-mail: wyl@cqu.edu.cn; Fax: +86 17830862118; Tel: +86 17830862118*

[b]*Key Laboratory of Biorheological Science and Technology (Chongqing University), Ministry of Education, Chongqing 400044, China*

† These authors contributed equally to this work and should be considered co-first authors.

antianxiety drugs, anti-inflammatory drugs, anticancer drugs, and so on.[29–33] However, these are mainly small molecule drugs, and their synthetic routes are relatively complex. In view of this, we probed the possibility of using PA as a raw material to prepare novel polymers with good biological activity, and we simultaneously streamline the preparation process. We have conducted preliminary explorations and verified the feasibility of this idea in a previous study. In this article, we will elaborate on our previous work.[34,35]

Herein, we chose PA and EDTAD as the raw materials to synthesize a novel piperazine polymer in a simple way. The antibacterial properties and biocompatibility of the obtained polymer were then evaluated to determine its potential application. In particular, the antibacterial activity of this novel polymer toward two reference strains, *E. coli* ATCC 25922 and *S. aureus* ATCC 6538, were investigated. Among the multitudinous bacteria that cause clinical infections, *S. aureus* is considered to be the most problematic, due to its high incidence in burn, traumatic and other types of wounds.[36,37] In addition to this, further evaluation of the biocompatibility (or cytotoxicity) of this novel polymer to osteoblasts was conducted. Ciprofloxacin, a widely used antibacterial agent that contains a piperazine unit, was selected as a control in these two important experiments.

2. Experimental section

2.1 Materials

The EDTAD, PA, Rhodamine-Phalloidin and 4′,6-diamidino-2-phenylindole (DAPI) were purchased from the Sigma-Aldrich Corporation and used without further treatment or purification. Dimethyl sulfoxide (DMSO) and anhydrous ethanol were purchased from the Chongqing Drug Stock Limited Company and dried on molecular sieve. A Cell Counting Kit (CCK-8) was supplied by Solarbio. The Dulbecco's Modified Eagle's Medium (DMEM)/F12, trypsin, and fetal bovine serum were purchased from the Gibco. *E. coli* and *S. aureus* were supplied by Beijing Centers for Disease Prevention and Control, were used as the model prokaryotic organism in this research. Bacteria were cultured in Luria–Bertani (LB) medium and grown aerobically at 37 °C until the mid-logarithmic growth phase was achieved. To carry out the following antibacterial activity tests, the bacteria suspension was diluted with LB medium to achieve a starting concentration of approximately 10^6 CFU mL^{-1}. The newborn SD rats were purchased from the Experiment Animal Center of Army Medical University.

2.2 Preparation of PE

PE was synthesized by a simple and fast method (Fig. 1). First, equimolar amounts of EDTAD and PA were dissolved in DMSO under nitrogen environment, respectively. Then, the solution containing EDTAD was added dropwise to the solution containing PA under nitrogen with magnetic stirring at 40 °C. After reacting for 24 h, the obtained mixed solution was added to an excess of anhydrous ethanol to produce precipitates, and subsequently vacuum dried to constant weight at room temperature.

2.3 Structural characterization

The FTIR spectra of EDTAD and PE were measured with KBr pellets, and recorded using a Perkin Elmer Spectrum GX model, the detection range was from 400 to 4000 cm^{-1}. ^{13}C NMR was performed on a Bruker AV-4500 nuclear magnetic resonance spectrometer and the dried samples were dissolved in D_2O. The contents of each element in PE were detected using a WACRO elemental analyzer, for which, the accuracy of analysis was C, H, and N $\leq$0.1%.

2.4 Thermal analysis

2.4.1 TGA analysis. The thermal stability of PE was characterized using a STA449C thermal analysis system (NETZSCH). The amount of PE for each measurement was about 10 $\pm$ 0.1 mg, and all of the measurements were performed under a Ar atmosphere with a gas flow and heated up from ambient temperature to 600 °C. The heating rates of 5°C min^{-1} was used, the temperature and weight changes of PE were recorded continuously.

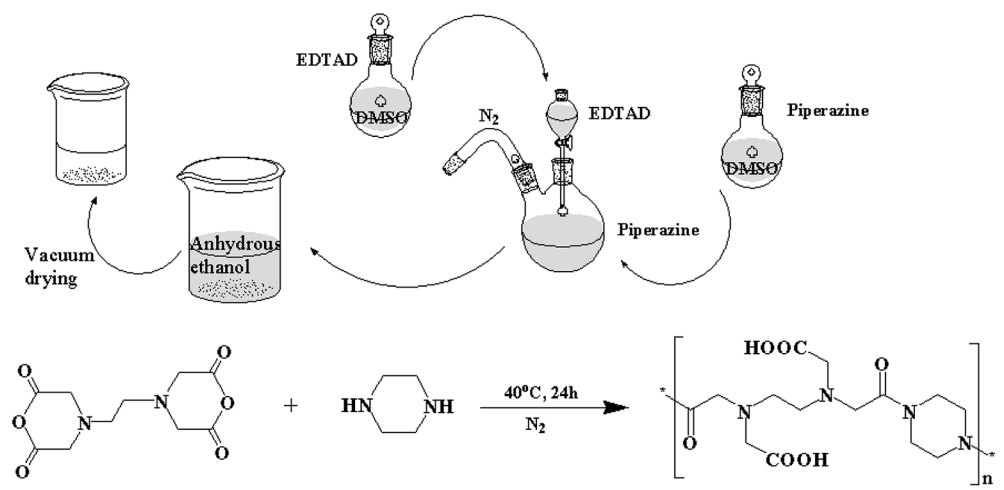

Fig. 1 The molecular structure of and synthetic routes for PE.

2.4.2 DSC analysis. PE of about 5 mg was encapsulated in Al pans and measured from two cyclic heating and cooling scans by differential scanning calorimeter (Perkin Elmer) under a dry nitrogen gas flow. The DSC measurement was performed at a heating and cooling rate of 10 °C min^{-1}.

2.5 Antibacterial activity tests

Several methods have been described in the literature to assess antimicrobial properties, such as the agar or disk diffusion test. The quantitative methods include: determination of minimum inhibitory concentration (MIC) and broth microdilution,[38–40] determination of colony forming units,[41–43] direct contact tests,[44,45] scanning electron microscopy (SEM) and transmission electron microscopy (TEM),[46–48] *etc.* In this study, we chose some of these methods to determine the antibacterial properties of PE.

2.5.1 Planktonic bacteria. The antibacterial activity of PE against *E. coli* and *S. aureus* in suspensions was evaluated. The MIC, growth curves, colony formation after treatment with different concentrations of PE, the morphology and internal structure of bacterial cells that were treated with PE at a certain concentration were investigated.

MIC is defined as the lowest concentration of a compound that will completely inhibit the visible growth of microorganisms after an overnight incubation. In this study, the microdilution method[49] was employed to evaluate the MIC of PE against *E. coli* and *S. aureus*. Ciprofloxacin, a commercially available and broad spectrum antibiotic, was selected as the standard for comparison. First, 200 μL of the PE and ciprofloxacin solutions at the initial concentrations were deposited in triplicate in the first column of a sterile 96-well plate. Then, 100 μL of the solutions containing PE or ciprofloxacin were transferred into the wells of the next column, which contained 100 μL of a sterile liquid medium, and then mixed sufficiently. This dilution process continued until the 10^{th} column was reached. Then, 100 μL of the bacterial suspension was added to each well, and the mixtures were incubated at 37 °C for 16–18 h. The MIC was the lowest concentration at which there was no visible growth, *i.e.*, there was no observed turbidity.

To investigate the bacteria colony formation after treatment with different concentrations of PE, 10 μL of the mixtures from the wells with no observed was used to coat plates. After incubating overnight at 37 °C, the colonies were counted. The concentrations of the selected wells were MIC, 2MIC and 4MIC. The bacteria before treatment was chosen as the control.

To better understand the antibacterial properties of PE, growth curves were performed for each strain. To start, different concentrations of PE and a certain concentration of ciprofloxacin were added into test tubes containing a certain concentration of a bacterial suspension. Then, the samples were incubated at 37 °C with agitation at 150 rpm for 10 h. The number of bacteria was determined at 0, 0.5, 1, 2, 4, 6, 8 and 10 h by collecting 90 μL samples at each time-point. These samples were transferred to a 96-well plate that had been prefilled with 10 μL of an MTT solution, and then incubated for another 3 h. After that, 100 μL of formazan was added to each well to sufficiently dissolve the crystals. The absorbance value of each well at 490 nm was measured by a microplate reader.

The antibacterial mechanism of PE against *E. coli* and *S. aureus* was further evaluated by SEM and TEM analysis. A certain concentration of PE solution was added to the bacterial suspension, and the PE concentration was adjusted to 1.17 μmol mL^{-1}. The mixtures were cultured under the same conditions used in the above antibacterial assay. After incubating for approximately 1 h, the PE-treated bacteria cells were collected and prepared for SEM and TEM analysis according to the procedure described in ref 50 and 51. For SEM, the micrographs of the bacteria cells were viewed at a 3.0 kV accelerating voltage on a ZEISS ULTRA 55, and a secondary electron image of the bacteria cells was collected at several magnifications to observe changes in the surface characteristics. For TEM, the bacteria cells were immersed in EPON (liquid epoxy) resin, and ultrathin sections were examined on a JEOL JEM 2100F microscope.

2.5.2 Adherent bacteria. To evaluate the antibacterial activity of PE against adherent bacteria, the bacteria suspension was first incubated in a sterile 24-well plate at 37 °C for approximately 3–4 h. Then, the wells were rinsed 3–4 times with sterile distilled water to remove the non-adherent bacteria. After that, 0.5 mL of PE solutions with different concentrations were added to the wells, and the 24-well plate was then incubated at 37 °C for another 0.5 h. After that, the PE solution was removed and the wells were again rinsed 3 times with sterile distilled water. After coloration with DAPI (0.5 μg mL^{-1}, in triple-distilled water), the 24-well plate was mounted on the motorized stage of the fluorescence microscope (Olympus Corporation) and the images were acquired.

2.6 Biocompatibility test

2.6.1 Cell culture. The mammalian cells chosen for this study were osteoblasts, which were isolated from newborn SD rat calvaria by an established method.[52] First, the cells were cultured in a DMEM/F12 medium, which contained 10% fetal bovine serum and a certain concentration of antibiotics. During this process, the culture medium was replaced every two days until it reached 80% confluence. Then, the cells were removed from the tissue culture flask and passaged in a new Petri dish. These cells were called P_1 (the first generation of cells). The third passage of cells were used for follow-up studies.[53]

2.6.2 Cell morphology. First, the above cells of a certain concentration were added into a sterile 24-well plate and then cultured in a three-gas cell incubator for 24 h. Second, the culture media containing different concentrations of PE, or a certain concentration of ciprofloxacin, were used to replace the initial culture medium, and then incubation continued for approximately 24 h. Finally, these culture media were discarded, and the nuclei and skeletons of the cells were stained for viewing. The specific process was as follows: (a) the cells were washed with phosphate buffered saline (PBS) 2–3 times. (b) The osteoblasts were fixed with an immunostaining fixative at 4 °C, and then the fixative was discarded after 30 minutes. (c) The cells were treated with 0.25% of TritonX-100 for another 10

minutes, and then washed with PBS approximately 3 times. (d) The cytoskeleton was stained with Rhodamine-Phalloidin at a concentration of 5 U mL^{-1}, and then incubated at 4 °C for approximately 12 h. (e) Washed again, and the nuclei were then stained with DAPI solution at a concentration of 0.5–10 μg mL^{-1} at room temperature for another 10 minutes (the whole process should be performed in the dark). (f) The cells were washed again, and then covered with an anti-fluorescence quenching sealing liquid. (g) Observations were made and photos were recorded.

2.6.3 Cell proliferation. Cell proliferation is another important physiological process that takes place after the initial contact between materials and cells. Cell proliferation is not only a direct reflection of cell survival after exposure to PE; it is also closely related to the subsequent functional expression of cells, such as maturity, differentiation and mineralization.[52] Therefore, the proliferation of osteoblasts was chosen to further evaluate the cytotoxicity of PE.

First, osteoblasts were seeded on a 96-well plate at a density of 3×10^4 per mL, cultured in DMEM/F12 supplemented with 10% fetal bovine serum and maintained in a controlled atmosphere for 24 h. After that, the culture medium was replaced by a special medium containing a certain concentration of PE or ciprofloxacin, and then continued to culture for approximately 2 days. This day was defined as "0". Beyond that, the culture medium was changed to the normal one, and the cell culture medium was renewed every 2 d. The number of osteoblasts was determined after 1, 4, and 7 d using CCK-8. The average osteoblast proliferation rate was the percentage increase in the osteoblast quantity per day, calculated according to eqn (1).

The average osteoblast proliferation rate:

$$\frac{P_2 - P_1}{P_1 \times \Delta t} \times 100\% \quad (1)$$

where P_1 and P_2 are the optical density (OD) values corresponding to culture times t_1 and t_2, respectively; Δt is the time interval between t_2 and t_1.[52]

2.7 Statistical analysis

All experiments were performed at least three times. Statistical comparisons were performed using SPSS software. The significant difference between two sets of data was considered when $p < 0.01$.

3. Results and discussion

The conjugation of PA and EDTAD was based on the reaction between the amino functional groups of PA and the acid anhydride groups of EDTAD. The synthetic route is shown in Fig. 1.

3.1 Structural characteristics of PE

FTIR is usually employed to detect structural changes in substances. That is because the various groups in the material have their own specific infrared absorption peaks. Fig. 2 shows the FTIR spectra of the PA, EDTAD and PE samples. From the photograph, it can be seen that PA has a visible absorption peak at 3360 cm^{-1}, which was assigned to the stretching vibration of –N–H bending (Fig. 2a). EDTAD showed two distinctive characteristic peaks at 1808 cm^{-1} and 1762 cm^{-1}, which were attributed to the high and low frequency absorption peaks of –C═O in the acid anhydride groups (Fig. 2b), respectively. After PA and EDTAD conjugation, the stretching vibration peak of –N–H was replaced by the –O–H absorption peak in the carboxyl groups of the side chains at 3430 cm^{-1}. This absorption peak showed a lower wave-number when compared to free –O–H, which indicated that there may be some hydrogen bond force in PE. Meanwhile, the characteristic peak for acid anhydride groups disappeared in PE, and instead there were two new absorption peaks, of which 1714 cm^{-1} was the characteristic –C═O absorption peak for carboxyl groups in the side chains, and 1639 cm^{-1} was the characteristic –C═O absorption peak for –C═O–N–. These results suggested that PE was synthesized successfully.

^{13}C NMR analysis was also employed to characterize the structure of PE, and the results are shown in Fig. 3. The peak at 41.34 ppm (pink) was attributed to the $-CH_2$ of PA. The peak at 44.44 ppm (yellow) was attributed to the $-CH_2$ of the EDTAD backbone. The peaks at 50.87 ppm (red) and 55.21 ppm (blue) were assigned to $-CH_2$ associated with imide bonds and carboxyl groups on the side chains of PE, respectively. In addition, the peaks appeared at 168.24 ppm (purple) and 171.87 ppm (green) correspond to the carbons atoms of the –C═O–N– and –COOH groups of PE. The above information from the ^{13}C NMR spectrum confirmed the successful synthesis of PE.

Next, elementary analysis was further performed to confirm the reaction between PA and EDTAD. As shown in Fig. 4, elemental analysis provides the information regarding the atoms constituting PE. As expected, there were four peaks corresponding to C, H, O and N. By integrating the area of each

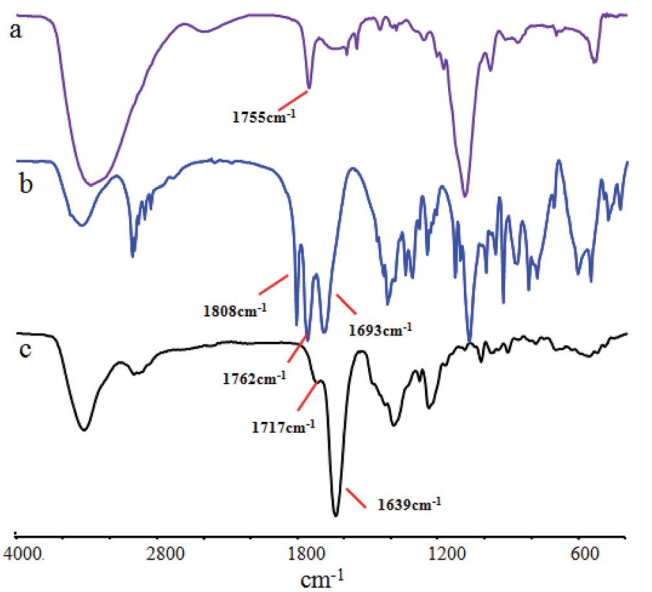

Fig. 2 The FTIR spectra of PA (a), EDTAD (b) and PE (c).

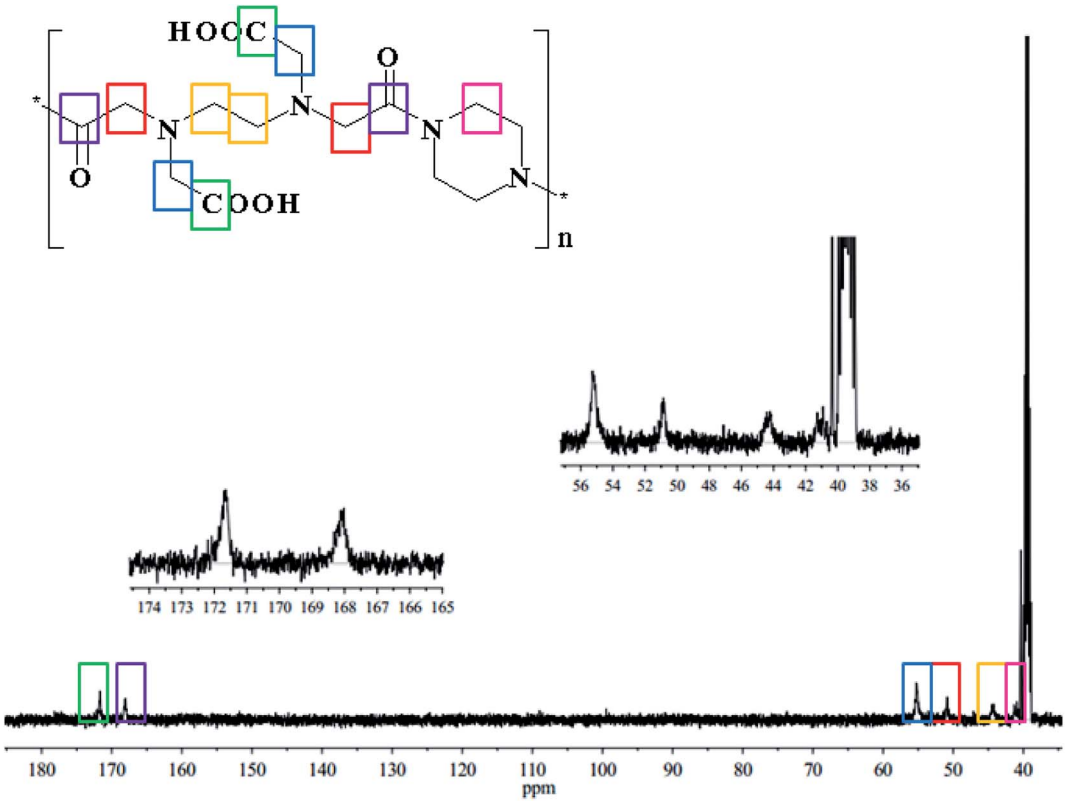

Fig. 3 ^{13}C NMR spectra of PE.

peak, the C/N ratio in PE was calculated to be 3.04. The C/N ratio in PA was approximately 1.71, while it was approximately 4.29 in EDTAD. From this information, it can be inferred that PA and EDTAD were reacted in an approximately 1 : 1 ratio, which is consistent with our raw material input ratio, and the structure of PE was as expected.

3.2 Thermal analysis

TGA results for PE are shown in Fig. 5. The curve could be divided into two regions. The first region occurred before 100 °C, which was attributed to the loss of water in PE. The second weight loss occurred at approximately 200–250 °C, and this high temperature mass loss is related to the degradation of PE.

Fig. 6 shows the DSC thermograms of PE after a second heating run. As shown in the figure, PE had a clear glass transition temperature of 50.09 °C, which is consistent with our previous study, and there was a complete phase transformation process at this point.[34] This result suggests that the pure piperazine polymer can be prepared through this simple and fast method.

3.3 Antibacterial activity

3.3.1 Planktonic bacteria. Our primary goal was to study the antibacterial activity all along the chemical pathway. Therefore, the antibacterial activity of PE against Gram-positive *S. aureus* and Gram-negative *E. coli* was tested in free and adherent states, respectively. The antibacterial activity results are as follows.

The MIC is defined as the lowest concentration of an antimicrobial compound that will inhibit the visible growth of a microorganism after overnight incubation. By using the microdilution method, the MIC of PE was found to be 1.17 μmol mL^{-1} against *E. coli* or *S. aureus* at a concentration of 10^6 CFU mL^{-1}. Meanwhile, at least 1.63 μmol mL^{-1} of ciprofloxacin was needed to inhibit the visible growth of *E. coli*, and the MIC of ciprofloxacin was approximately 3.26 μmol mL^{-1} against *S. aureus*, as shown in Table 1. These results indicated that a certain concentration of PE could inhibit the growth of bacteria, and its antibacterial ability may be better than that of ciprofloxacin.

Fig. 7 and Fig. 8 show the characterizations of *E. coli* and *S. aureus* colony formation after treatment with different concentrations of PE. From the figures, it can be seen that PE showed a strong antibacterial effect in a dose-dependent manner. In other words, as the concentration of PE increased, the number of colonies on the plates gradually decreased. Interestingly, at a higher concentration of 4MIC, PE killed the *E. coli* completely, and there were no colonies generated on the plate, as shown in Fig. 7d. However, when the *S. aureus* was exposed to the same concentration of PE, a small number of colonies were observed on the plate, as shown in Fig. 8d. These results indicated that PE reduced the viabilities of both *E. coli* and *S. aureus*, but the antibacterial effect of PE against *E. coli* was much better. This may be explained by the different cell wall structures of *S. aureus* and *E. coli.*

To further evaluate the antibacterial ability of PE, the growth inhibitions of *E. coli* and *S. aureus* were tested with different

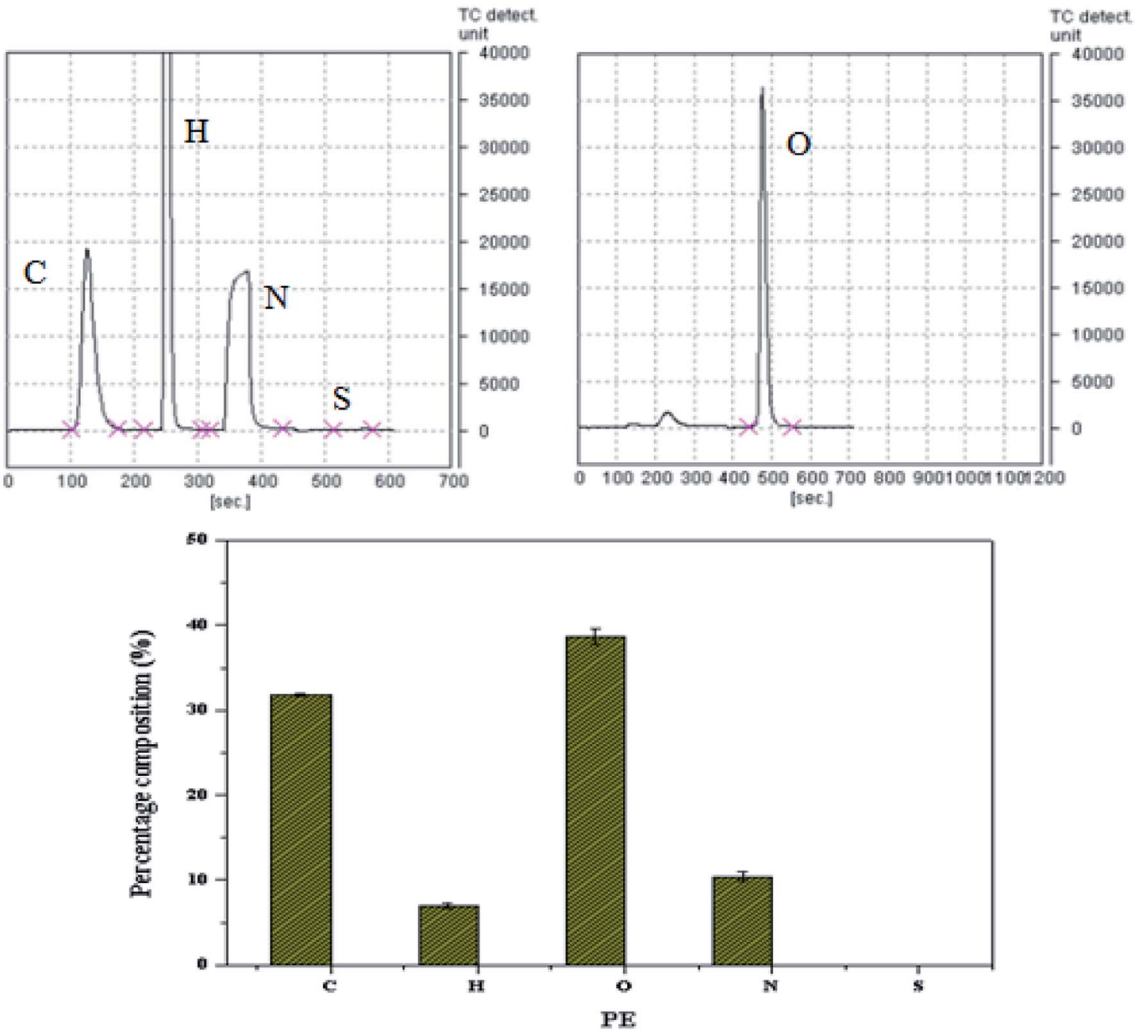

Fig. 4 The elementary analysis of PE.

concentrations of PE. From Fig. 9, it can be seen that the antibacterial ability of PE against the planktonic bacteria was similar to that of ciprofloxacin and was concentration-dependent. Specifically, in the initial contact stage, the MIC of PE reduced the number of planktonic bacteria to some extent, then this phenomenon disappeared soon afterwards and resulted in an overall growth inhibition. This unreasonable

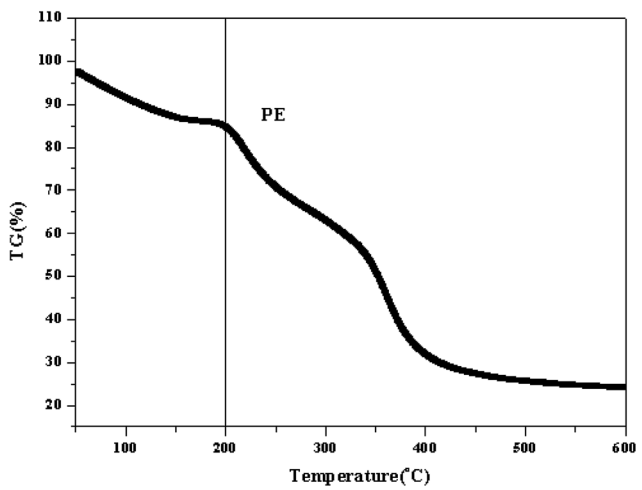

Fig. 5 The TGA curve of PE.

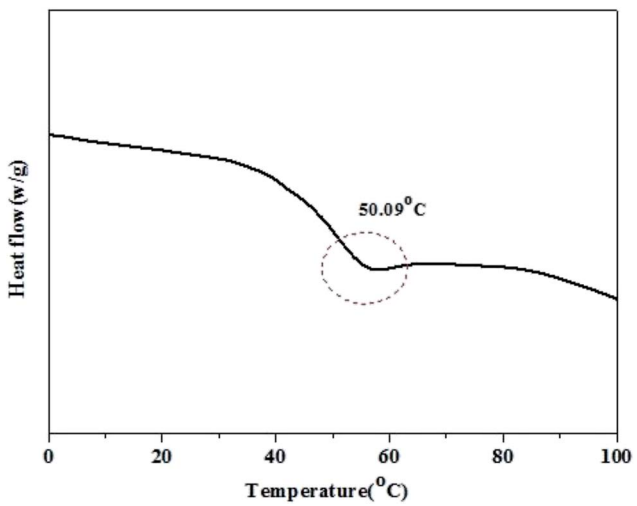

Fig. 6 DSC thermograms of PE.

Table 1 The MIC of PE to bacteria

Bacterial strain	MIC (μmol mL^{-1})	
	PE[a]	Ciprofloxacin[b]
E. coli ATCC 25922	1.17	1.63
S. aureus ATCC 6538	1.17	3.26

[a] M_n (PE) ≈ 5341 g mol^{-1}, which was calculated by EC. [b] M_n (ciprofloxacin) = 331.34 g mol^{-1}.

phenomenon was attributed to the insufficient mixing during this period, which may have caused the concentration of PE in some areas to be greater than the MIC value, so the number of bacteria slightly decreased. Comparing the growth inhibition curves of *E. coli* and *S. aureus*, it was found that the *E. coli* could be killed completely by PE at a concentration of 4MIC, while there were still some *S. aureus* alive after treatment with the same concentration of PE. This result was consistent with the colony formation, which suggested that PE showed better antibacterial activity against Gram-negative bacteria while compared to Gram-positive bacteria.

Toxic effects are usually accompanied by changes in bacterial surface morphology, and the changes that occur inside the bacteria can further explain the material's mechanism of action. For this study, SEM was utilized to identify the morphology and membrane integrity of both the *E. coli* and *S. aureus* cells after treatment with PE for 1 h, and the results are shown in Fig. 10. In detail, the *E. coli* in the control group were rodlike in shape, and the surfaces were smooth and relatively intact. However, after exposure to an aqueous PE solution for 1 h, the *E. coli* cells suffered from a change in cell shape. Most of the bacteria changed from a rodlike shape to an irregular shape with severe membrane damage and cytoplasm leakage. Surprisingly, this phenomenon was not as obvious in the *S. aureus* experimental group. Compared to the *S. aureus* control, the bacteria in both groups were typically round in shape, but the surfaces of the *S. aureus* in the experimental group were rough, and even had a small number of holes. These results indicated that a certain concentration of PE could change the morphology of *E. coli* and *S. aureus* cells, which might eventually lead to growth inhibition or death of the bacteria, *S. aureus* was less susceptible to PE when compared to *E. coli*, and this result

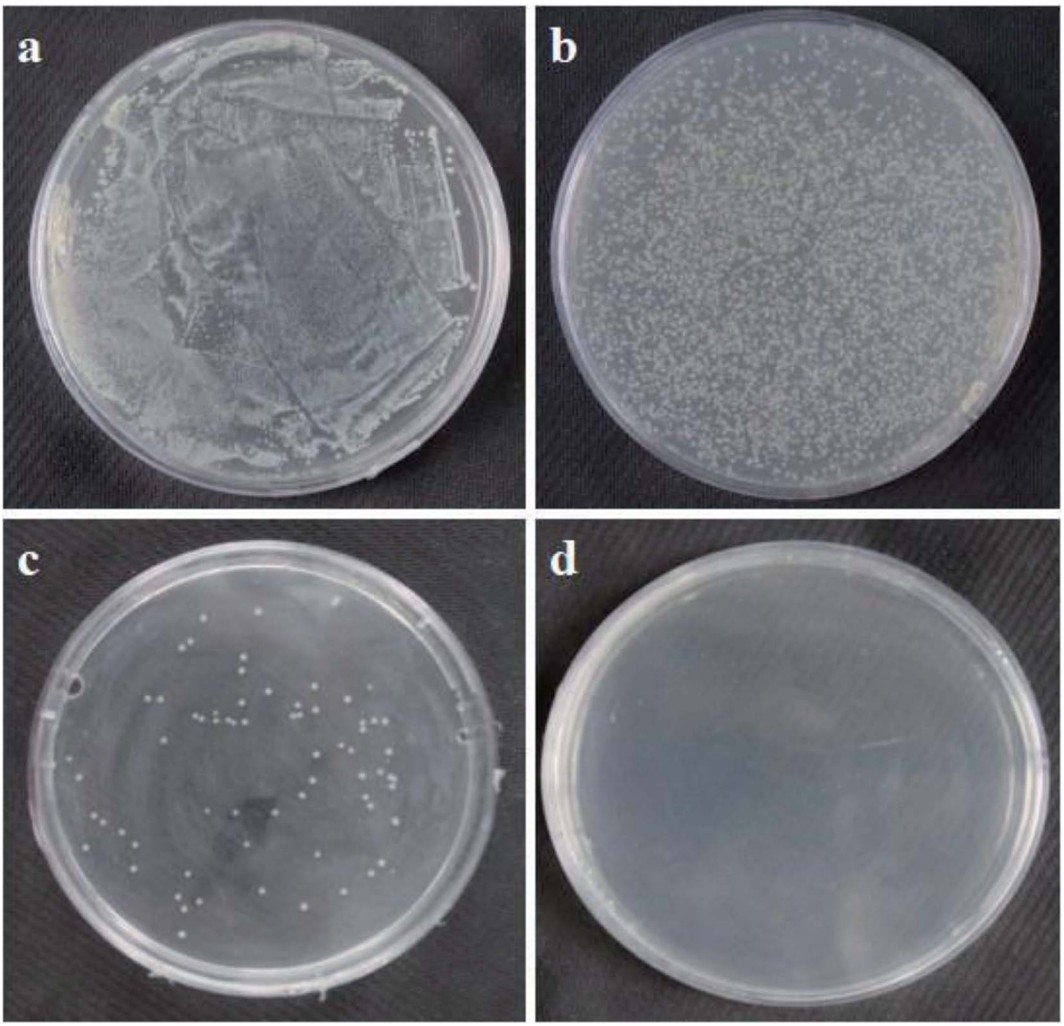

Fig. 7 Colony formation of *E. coli* treated with PE ((a) control, (b) MIC, (c) 2 MIC, (d) 4 MIC).

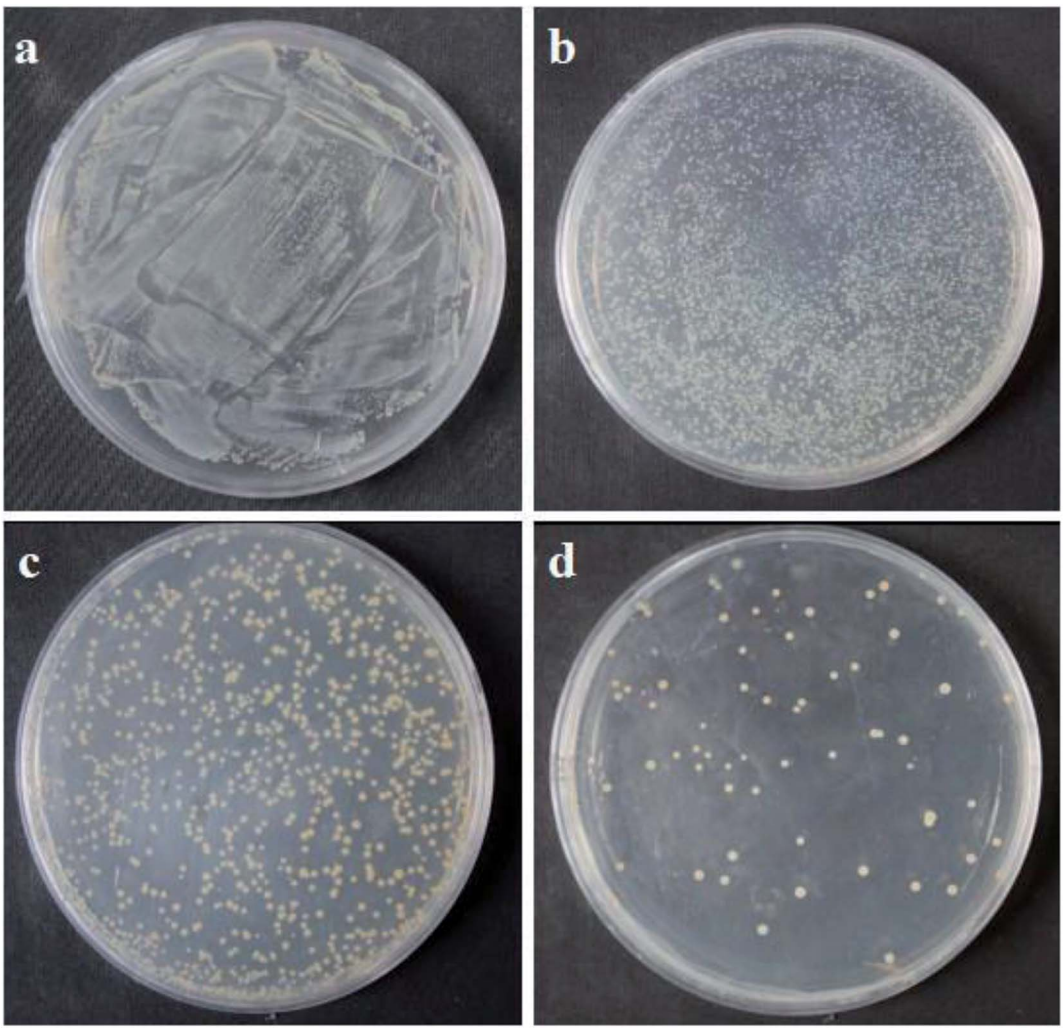

Fig. 8 Colony formation of *S. aureus* treated with PE ((a) control, (b) MIC, (c) 2 MIC, (d) 4 MIC).

was consistent with the colony formation results. Furthermore, TEM was also employed to study the antibacterial mechanism of PE. It can be seen from Fig. 10 that both the *E. coli* and *S. aureus* in the control groups underwent division and proliferation, and the distribution of the cell contents was uniform. However, after PE treatment for an hour, both bacteria lost the ability to divide and proliferate, and some cytoplasmic deletions were also observed in the experimental groups. These results further confirm our speculation that the PE could not only destroy the cell wall membrane but also cause the loss of cell contents, thereby exerting its antibacterial effect.

3.3.2 Adherent bacteria. It is well known that once the bacteria adhere to the surfaces of the materials, the effect of compounds on the bacteria will be greatly reduced. Therefore, we investigated the effects of different concentrations of PE on the adhered bacteria, and the results are shown in Fig. 11.

After an adhesion time of 3–4 h, the fluorescence microscopy images showed a great number of bacteria covering the entire bottom portion of the blank orifice plates. However, when treated with a certain concentration of PE for approximately 0.5 h, an absence of bacteria was observed, and the number of missing bacteria showed a strong dose-dependency. However, it was noteworthy that even when treated with 4MIC PE, there was still a considerable amount of adhered bacteria at the bottom of the orifice plates. These results suggested that the antibacterial effect of PE on adhered bacteria was weaker than that of Planktonic bacteria, which is similar to the results for antibacterial materials currently reported in most of the literature. Further research is needed to study this subject, and hopefully the activity toward adhered bacteria can be improved.

3.4 Biocompatibility test

Different kinds of cells have different cell shapes, depending on their structures, surface tension or the influence of external environments. It is important that the morphology of the cells is closely related to their life activities and functions. Therefore, the effect of PE on the shapes of osteoblasts could be proof of its cytotoxicity. Fig. 12 shows the morphology of osteoblasts after 24 h of different drug treatments. As seen from the pictures, the osteoblasts without any drug treatment were well spread out and contained a large number of protein fibers (Fig. 12c). However, a variety of changes were observed in the other groups after a 24 h drug treatment. For the PE treatment groups, there

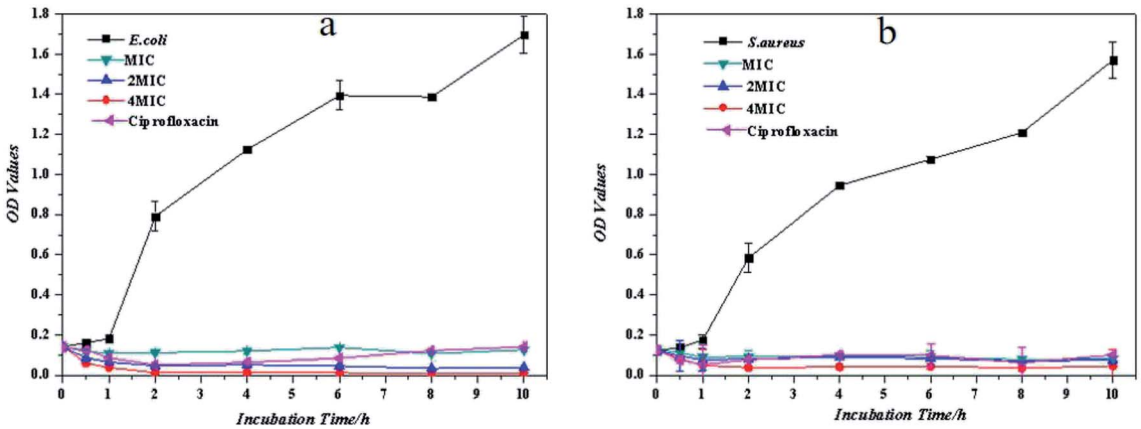

Fig. 9 Growth curves for *E. coli* (a) and *S. aureus* (b) treated with PE.

was a concentration dependence. When treated with the MIC of PE, the effects on the osteoblasts' morphology were not obvious (Fig. 12e). However, as the concentration of PE increased, its influence on cell morphology increased gradually. Specifically, as the concentration increased, the osteoblasts decreased, the spreading was incomplete and the number of F-actin fibers decreased (Fig. 12b, d, and e). Surprisingly, this phenomenon was more pronounced in the ciprofloxacin treatment group (Fig. 12a). These results indicated that when the concentration of PE reached a certain level, it produced a certain toxicity in osteoblasts.

As an effective method for measuring the number of cells, CCK-8 has been widely used in several fields, such as detecting anticancer drug cytotoxicity, or the cell proliferation assays induced by drugs or cytokines. In this study, CCK-8 was selected to evaluate the effect of PE on the osteoblasts' proliferation rate,

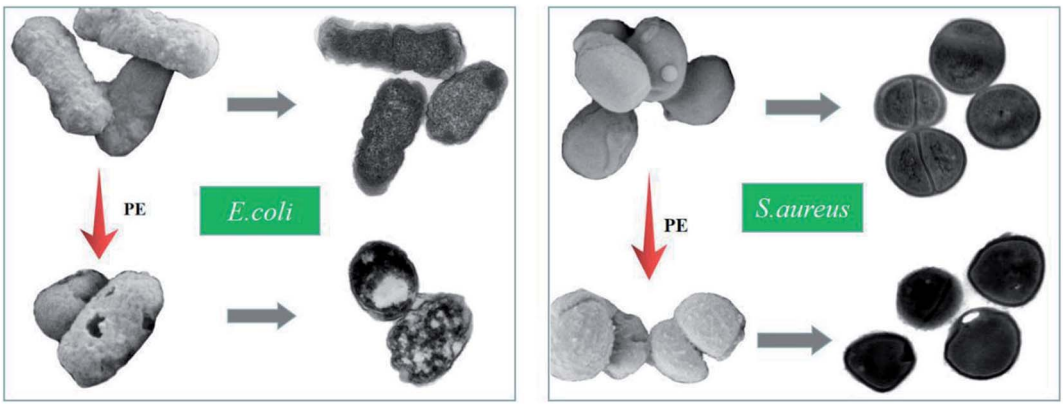

Fig. 10 The electron microscopy images of bacteria.

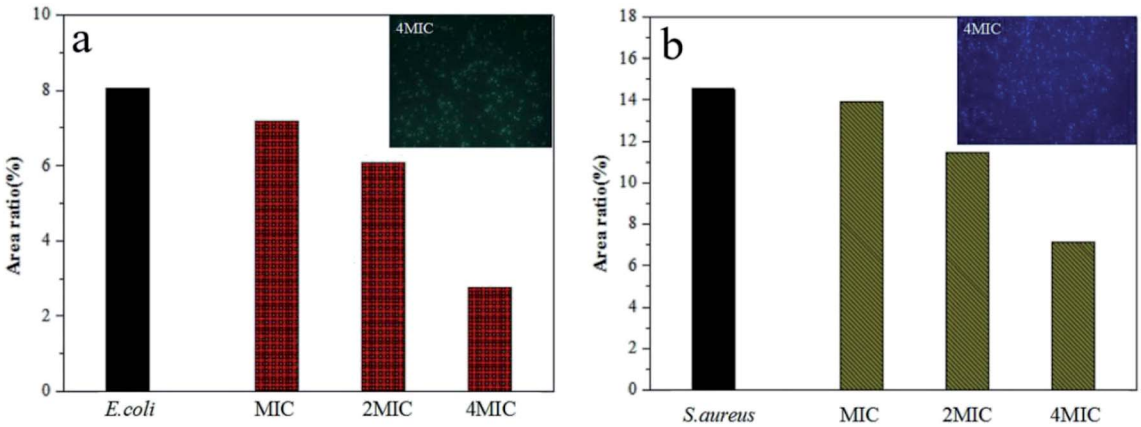

Fig. 11 The rapid killing effect of adhered *E. coli* (a) and *S. aureus* (b) by PE ×200.

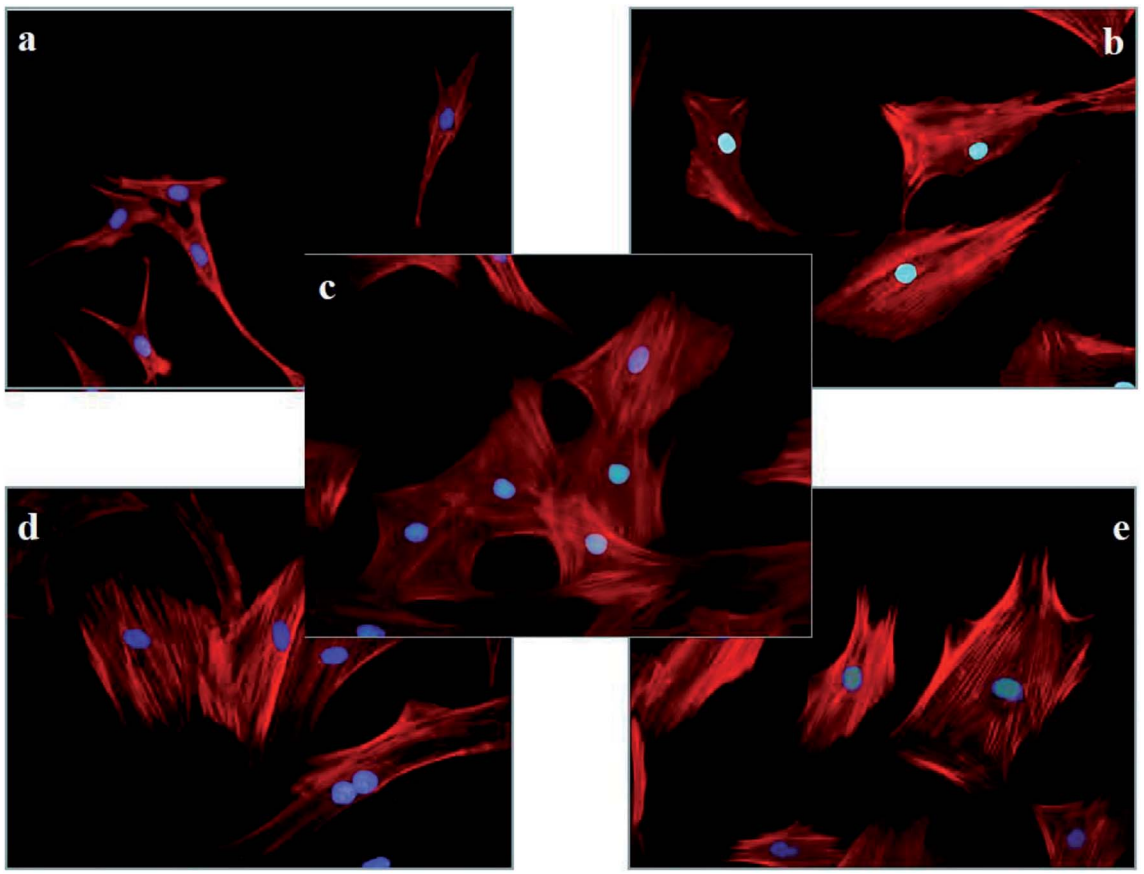

Fig. 12 The morphology of rat calvarial osteoblasts treated with different materials for 24 h (×400) ((a) ciprofloxacin, (b) PE-4MIC, (c) control, (d) PE-2MIC, (e) PE-MIC).

and the results are shown in Table 2. From the control group, it can be seen that after a 24 h of adapting period, the osteoblasts began to proliferate slowly. In 1–4 days, the average proliferation rate increased significantly and achieved a maximum. Then, after 4 days, the average cell proliferation rate was reduced. This phenomenon can be explained by contact inhibition due to the large cell density during this period. However, all of the experimental groups showed a reduced proliferation rate on the first day, indicating that neither ciprofloxacin nor PE showed some toxicity to osteoblasts. Then, in 1–4 days, the average proliferation rates of the experimental groups increased and achieved a maximum value. After that, the average osteoblast proliferation rates between days 4–7 decreased as in the control group. Specifically, the PE-treated groups showed a lower toxicity toward osteoblasts than that of ciprofloxacin at the same molarity. In view of this, the subsequent work should focus on modifying PE to reduce its cytotoxicity.

Table 2 The average proliferation rate (%) of rat calvarial osteoblasts treated with PE

	Average proliferation rate (%)		
Contents	0–1 d	1–4 d	4–7 d
Control	2.63	35.89	13.18
Ciprofloxacin	−4.30	20.11	14.83
PE	−4.06	23.47	14.69

4. Conclusions

In this paper, a novel piperazine polymer, PE, was synthesized successfully through a simple and fast method. In addition, the overall reaction conditions were mild and required no catalyst. The thermal stability of the as-prepared PE was estimated from the results of TGA and DSC, which showed that the thermal decomposition and glass transition temperatures of PE were approximately 200–250 °C and 50 °C, respectively. When the antibacterial material is applied to an infected part of the body, it may also have a certain toxicity to the eukaryotic cells, while achieving the effective killing of bacteria. Based on this observation, the antimicrobial properties and biocompatibility of PE were studied in this paper. For the antibacterial experiments, PE showed significant antibacterial activity against *E. coli* and *S. aureus*. When combining the experimental results of the antimicrobial test with biocompatibility test, there was a bold prediction. There may be a threshold value for damage to the bacteria and osteoblasts when treated with PE, and the damage threshold for osteoblasts was higher than that for bacteria. The reason for this difference may be related to the size of the osteoblasts and bacteria. That is, when treating osteoblasts and bacteria with the same concentration of PE, the charge density

and number of active groups relative to the osteoblasts were both less than that of the bacteria. Therefore, compared with osteoblasts, the inhibition and killing of bacteria was much greater. These results indicated that the obtained bioactive piperazine polymer may be an excellent candidate for biomedical applications, especially biomaterial applications, due to its antibacterial activity and biocompatibility. However, further investigations on the mechanism of action and the modification of PE to further reduce its cytotoxicity are required.

Conflicts of interest

There are no conflicts to declare.

Acknowledgements

This study was funded by the National Natural Science Foundation (Project No. 51808086, 11532004), Visiting Scholar Foundation of Key Laboratory of Biorheological Science and Technology (Chongqing University), Ministry of Education (Project No. CQKLBST-2017-010), Natural Science Fund Foundation of Chongqing Science and Technology Commission (Project No. cstc2018jcyjAX0078, cstc2018jcyjAX0286), China Academy of Engineering Consulting Research Project (No. 2018-XZ-CQ-3) and the Scientific Research Foundation of Sichuan University of Science & Engineering (Project No. 2016RCL06).

References

1 I. Molina, M. Mari, J. V. Martínez, E. Novella-Maestre, N. Pellicer and J. Peman, Bacterial and fungal contamination risks in human oocyte and embryo cryopreservation: open versus closed vitrification systems, *Fertil. Steril.*, 2016, **106**, 127–132.

2 J. S. Martinez, K. D. Kelly, Y. E. Ghoussoub, J. D. Delgado, T. C. S. III Keller and J. B. Schlenoff, Cell resistant zwitterionic polyelectrolyte coating promotes bacterial attachment: an adhesion contradiction, *Biomater. Sci.*, 2016, **4**, 689.

3 P. Gupta, N. Bairagi, R. Priyadarshini, A. Singh, D. Chauhan and D. Gupta, Bacterial contamination of nurses' white coats made from polyester and polyester cotton blend fabrics, *J. Hosp. Infect.*, 2016, **94**, 92–94.

4 M. Lee, H. Kim, J. Seo, S. Kang, J. Jang, Y. Lee and J. H. Seo, Surface zwitterionization: effective method for preventing oral bacterial biofilm formation on hydroxyapatite surfaces, *Appl. Surf. Sci.*, 2018, **427**, 517–524.

5 X. L. Luo, H. C. Wu, C. Y. Tsao, Y. Cheng, J. Betz, G. F. Payne, G. W. Rubloff and W. E. Bentley, Biofabrication of stratified biofilm mimics for observation and control of bacterial signaling, *Biomaterials*, 2012, **33**, 5136–5143.

6 M. Zilberman and J. J. Elsner, Antibiotic-eluting medical devices for various applications, *J. Controlled Release*, 2008, **130**, 202–215.

7 L. C. Xu and C. A. Siedlecki, Submicron-textured biomaterial surface reduces staphylococcal bacterial adhesion and biofilm formation, *Acta Biomater.*, 2012, **8**, 72–81.

8 G. Cheng, Z. Zhang, S. Chen, J. D. Bryers and S. Jiang, Inhibition of bacterial adhesion and biofilm formation on zwitterionic surfaces, *Biomaterials*, 2007, **28**, 4192–4199.

9 P. Liu, Y. S. Hao, C. Y. Zhao, Y. Ding and K. Cai, Surface modification of titanium substrates for enhanced osteogenetic and antibacterial properties, *Colloids Surf., B*, 2017, **160**, 110–116.

10 Y. Pan, Z. X. Yu, H. Shi, Q. Chen, G. Y. Zeng, H. H. Di, X. Q. Ren and Y. He, A novel antifouling and antibacterial surface-functionalized PVDF ultrafiltration membrane via binding Ag/SiO_2 nanocomposites, *J. Chem. Technol. Biotechnol.*, 2017, **92**, 562–572.

11 V. P. Parvathi, T. Jaiakumar, M. Umadevi, J. Mayandi and G. V. Sathe, Synergistic effect of MgO/Ag co-doping on TiO_2 for efficient antibacterial agents, *Mater. Lett.*, 2016, **184**, 82–87.

12 M. Matet, M. C. Heuzey and A. Ajji, Morphology and antibacterial properties of plasticized chitosan/metallocene polyethylene blends, *J. Mater. Sci.*, 2014, **49**, 5427–5440.

13 M. T. EI-Sayed, S. Suzen, N. Altanlar, K. Ohlsen and A. Hilgeroth, Discovery of bisindolyl-substituted cycloalkane-anellated indoles as novel class of antibacterial agents against S. aureus and MRSA, *Bioorg. Med. Chem. Lett.*, 2016, **26**, 218–221.

14 Y. Lu, D. L. Sloberg and A. Shah, Nitric Oxide-Releasing Amphiphilic Poly(amidoamine)(PAMAM) Dendrimers as Antibacterial Agents, *Biomacromolecules*, 2013, **14**, 3589–3598.

15 L. Z. Zhao, P. K. Chu, Y. M. Zhang and Z. F. Wu, Antibacterial coatings on titanium implants, *J. Biomed. Mater. Res., Part B*, 2009, **91**, 470–480.

16 Q. H. Zhang, H. L. Liu, X. Chen, X. L. Zhan and F. Q. Chen, Preparation, surface properties, and antibacterial activity of a poly(dimethyl siloxane) network containing a quaternary ammonium salt side chain, *J. Appl. Polym. Sci.*, 2015, **132**, 5–8.

17 D. Zhu, H. H. Cheng, J. N. Li, W. W. Zhang, Y. Y. Shen, S. J. Chen, Z. H. Ge and S. G. Chen, Enhanced water-solubility and antibacterial activity of novel chitosan derivatives modified with quaternary phosphonium salt, *Mater. Sci. Eng., C*, 2016, **61**, 79–84.

18 S. Ferraris, M. Miola, A. Cochis, B. Azzimonti, L. Rimondini, E. Prenesti and E. Verne, In situ reduction of antibacterial silver ions to metallic silver nanoparticles on bioactive glasses functionalized with polyphenols, *Appl. Surf. Sci.*, 2017, **396**, 461–470.

19 A. R. Unnithan, N. A. M. Barakat and T. Pichiah, Wound-dressing materials with antibacterial activity from electrospun polyurethane–dextran nanofiber mats containing ciprofloxacin HCl, *Carbohydr. Polym.*, 2012, **90**, 1786–1793.

20 D. Jabes, The antibiotic R&D pipeline: an update, *Curr. Opin. Microbiol.*, 2011, **14**, 564–569.

21 E. R. Kenawy, S. D. Worley and R. Broughton, The chemistry and applications of antimicrobial polymers: a state-of-the-art review, *Biomacromolecules*, 2007, **8**, 1359–1384.

22 A. Som, S. Vemparala, I. Ivanov and G. N. Tew, Synthetic mimics of antimicrobial peptides, *Biopolymers*, 2008, **90**, 83–93.
23 M. Zasloff, Antimicrobial peptides of multicellular organisms, *Nature*, 2002, **415**, 389–395.
24 M. Taniguchi, J. Kawabe, R. Toyoda, T. Namae, A. Ochiai, E. Saitoh and T. Tanaka, Cationic peptides from peptic hydrolysates of rice endosperm protein exhibit antimicrobial, LPS-neutralizing, and angiogenic activities, *Peptides*, 2017, **97**, 70–78.
25 M. Kalle, P. Papareddy, G. Kasetty, M. J. A. van der Plas, M. Mörgelin, M. Malmsten and A. Schmidtchen, A Peptide of Heparin Cofactor II Inhibits Endotoxin-Mediated Shock and Invasive Pseudomonas aeruginosa Infection, *PLoS One*, 2014, **9**, e102577.
26 S. Y. Wang, Y. M. Li, R. Zhao, T. F. Jin, L. Zhang and X. Li, Chitosan surface modified electrospun poly(ε-caprolactone)/carbon nanotube composite fibers with enhanced mechanical, cell proliferation and antibacterial properties, *Int. J. Biol. Macromol.*, 2017, **104**, 708–715.
27 J. H. Park, G. Saravanakumar, K. Kim and I. C. Kwon, Targeted delivery of low molecular drugs using chitosan and its derivatives, *Adv. Drug Delivery Rev.*, 2010, **62**, 28–41.
28 Q. F. Dang, K. Liu and C. S. Liu, Preparation, characterization, and evaluation of 3,6-O-N-acetylethylenediamine modified chitosan as potential antimicrobial wound dressing material, *Carbohydr. Polym.*, 2018, **180**, 1–12.
29 L. Li, Z. Li, N. Guo, J. Jin, R. Du, J. Liang, X. Wu and X. Wang, Synergistic activity of 1-(1-naphthylmethyl)-piperazine with ciprofloxacin against clinically resistant Staphylococcus aureus, as determined by different methods, *Lett. Appl. Microbiol.*, 2011, **52**, 372–378.
30 B. R. Raajaraman, N. R. Sheela and S. Muthu, Investigation on 1-Acetyl-4-(4-hydroxyphenyl) piperazine an anti-fungal drug by spectroscopic, quantum chemical computations and molecular docking studies, *J. Mol. Struct.*, 2018, **1173**, 583–595.
31 D. M. da Silva, G. Sanz, B. G. Vaz, F. S. de Carvalho, L. M. Liao, D. R. de Oliveira, L. K. de Silva Moreira and C. S. Cardoso, Tert-butyl 4-((1-phenyl-1H-pyrazol-4-yl) methyl) piperazine-1-carboxylate (LQFM104) – new piperazine derivative with antianxiety and antidepressant-like effects: putative role of serotonergic system, *Biomed. Pharmacother.*, 2018, **103**, 546–552.
32 D. P. B. Silva, I. F. Florentino, L. P. Oliveira, R. C. Lino, P. M. Galdino, R. Menegatti and E. A. Costa, Anti-nociceptive and anti-inflammatory activities of 4-[(1-phenyl-1H-pyrazol-4-yl) methyl] 1-piperazine carboxylic acid ethyl ester: a new piperazine derivative, *Pharmacol., Biochem. Behav.*, 2015, **137**, 86–92.
33 E. X. She and Z. Hao, A novel piperazine derivative potently induces caspase-dependent apoptosis of cancer cells via inhibition of multiple cancer signaling pathways, *Am. J. Transl. Res.*, 2013, **5**, 622–633.
34 J. X. Sun, Y. L. Wang and S. H. Dou, A novel positively thermo-sensitive hydrogel based on ethylenediaminetetraacetic dianhydride and piperazine: design, synthesis and characterization, *Chin. Chem. Lett.*, 2012, **23**, 97–100.
35 M. L. Zhang, Y. L. Wang, J. X. Sun, J. C. Wu, W. W. Yan and Y. X. Zheng, Design and Synthesis of Novel Piperazine Derivatives with High Antibacterial Activity, *Chem. Lett.*, 2013, **42**, 227–228.
36 J. Dissemond, E. N. Schmid, S. Esser, M. Witthoff and M. Goos, Bakterielle Kolonisation chronischer Wunden, *Der Hautarzt*, 2004, **55**, 280–288.
37 P. G. Bowler, B. I. Duerden and D. G. Armstrong, Wound microbiology and associated approaches to wound management, *Clin. Microbiol. Rev.*, 2011, **14**, 244–269.
38 D. Xie, Y. Weng, X. Guo, J. Zhao, R. L. Gregory and C. Zheng, Preparation and evaluation of a novel glass-ionomer cement with antibacterial functions, *Dent. Mater.*, 2011, **27**, 487–496.
39 B. A. Sevinç and L. Hanley L, Antibacterial activity of dental composites containing zinc oxide nanoparticles, *J. Biomed. Mater. Res., Part B*, 2010, **94**, 22–31.
40 F. Li, M. D. Weir, A. F. Fouad and H. H. K. Xu, Time-kill behaviour against eight bacterial species and cytotoxicity of antibacterial monomers, *J. Dent.*, 2013, **41**, 881–891.
41 L. Cheng, K. Zhang, M. A. S. Melo and M. D. Weir, Anti-biofilm dentin primer with quaternary ammonium and silver nanoparticles, *J. Dent. Res.*, 2014, **91**, 598–604.
42 F. Li, J. Chen, Z. Chai, L. Zhang, Y. Xiao, M. Fang and S. Ma, Effects of a dental adhesive incorporating antibacterial monomer on the growth, adherence and membrane integrity of Streptococcus mutans, *J. Dent.*, 2009, **37**, 289–296.
43 L. Cheng, M. D. Weir, P. Limkangwalmongkol, G. D. Hack, H. H. K. Xu, Q. M. Chen and X. D. Zhou, Tetracalcium phosphate composite containing quaternary ammonium dimethacrylate with antibacterial properties, *J. Biomed. Mater. Res., Part B*, 2012, **100**, 726–734.
44 S. E. Elsaka, I. M. Hamouda and M. V. Swain, Titanium dioxide nanoparticles addition to a conventional glass-ionomer restorative: influence on physical and antibacterial properties, *J. Dent.*, 2011, **39**, 589–598.
45 N. Beyth, Y. Houri-Haddad, L. Baraness-Hadar, I. Yudovin-Farber, A. J. Domb and E. I. Weiss, Surface antimicrobial activity and biocompatibility of incorporated polyethylenimine nanoparticles, *Biomaterials*, 2008, **29**, 4157–4163.
46 F. Li, Z. G. Chai and M. N. Sun, Anti-biofilm effect of dental adhesive with cationic monomer, *J. Dent. Res.*, 2009, **88**, 372–376.
47 T. P. T. Cushnie, N. H. O'Driscoll and A. J. Lamb, Morphological and ultrastructural changes in bacterial cells as an indicator of antibacterial mechanism of action, *Cell. Mol. Life Sci.*, 2016, **73**, 4471–4492.
48 D. Sun, D. H. Xu and C. G. Yanget, An investigation of the antibacterial ability and cytotoxicity of a novel cu-bearing 317L stainless steel, *Sci. Rep.*, 2016, **6**, 29244.
49 R. Reynolds, J. Shackcloth, D. Felmingham and A. Macgowan, Comparison of BSAC agar dilution and NCCLS broth microdilution MIC methods for in vitro

susceptibility testing of Streptococcus pneumoniae, Haemophilus influenzae and Moraxella catarrhalis: the BSAC Respiratory Resistance Surveillance Programme, *J. Antimicrob. Chemother.*, 2003, **52**, 925–930.

50 M. Torrent, S. Navarro, M. Moussaoui, M. V. Nogues and E. Boix, Eosinophil cationic protein high-affinity binding to bacteria-wall lipopolysaccharides and peptidoglycans, *Biochemistry*, 2008, **47**, 3544–3555.

51 M. Torrent, B. G. De la Torre, V. M. Nogues and D. Andreu, Bactericidal and membrane disruption activities of the eosinophil cationic protein are largely retained in an N-terminal fragment, *Biochem. J.*, 2009, **421**, 425–434.

52 P. G. Robey and J. D. Ternube, Human bone cells in vitro, *Calcif. Tissue Int.*, 1985, **37**, 453–460.

53 Y. X. Li, B. B. Zhang, C. S. Ruan and P. P. Wang, Synthesis, characterization, and biocompatibility of a novel biomimetic material based on MGF-Ct24E modified poly(D, L-lactic acid), *J. Biomed. Mater. Res., Part A*, 2015, **100**, 3496–3502.